IEEE Access
Multidisciplinary ⋮ Rapid Review ⋮ Open Access Journal

Received September 27, 2020, accepted October 1, 2020, date of publication October 14, 2020, date of current version October 23, 2020.

Digital Object Identifier 10.1109/ACCESS.2020.3030936

Principle of Optimal Voltage Regulation and Energy-Saving for Induction Motor With Unknown Constant-Torque Working Condition

ZHONG BIN[1], MA LILI[2], AND DONG HAO[1]
[1]School of Mechanical Engineering, Chengdu University, Chengdu 610106, China
[2]College of Equipment Management and Support, Engineering University of PAP, Xi'an 710086, China

Corresponding author: Zhong Bin (zhongbinchina@163.com)

This work was supported by the National Natural Science Foundation of China under Grant 11802041.

ABSTRACT To achieve optimal voltage regulation and energy savings of an AC induction motor operating under constant-torque and variable-working-load conditions, and consider a motor's T-type and Γ-type equivalent circuit, the copper and iron losses of the stator were regarded as invariable losses that were only related to the stator voltage, and the copper losses of the rotor were regarded as variable losses that varied with the load torque. The total electrical loss formula and the optimal voltage regulation formula for the motor were deduced. The formulas revealed that the total electrical loss of the motor was affected by the stator voltage and the rotor load torque, and the optimal voltage regulation changed exponentially with the load torque of the motor. The calculation results of an engineering example showed that when $s = 0.01$–0.03 and the motor operated stably, the motor load torque error was not more than 1.8 N·m based on the exact and approximate solutions of the slip s. The total electrical loss showed almost no calculation error when the working voltage of the motor was higher than 230 V. The optimal voltage regulation and its error increased with the increase in the motor load torque, but within the working voltage range of the motor, the optimal voltage regulation error did not exceed 6 V. The total electrical loss with the optimal voltage regulation mode and a variable load torque was less than the total electrical loss of a 380- or 220-V constant driving mode. With the increase in the load rate, the total electrical loss increased. When the motor's load did not exceed the medium load and the motor operated with optimal voltage regulation, the energy-saving effect was significant. In particular, when the motor operated without a load, the total electrical loss was almost 0.

INDEX TERMS Induction motor, constant-torque working condition, equivalent circuit, total electrical loss, optimal voltage regulation, energy-saving.

I. INTRODUCTION

If the load torque driven by the AC induction motor (hereinafter referred to as motor) is unknown and has a wide load-torque range, when selecting the motor, the rated power of the motor is generally determined according to the actual maximum load torque driven [1], [2]. For instance, to adapt to the hoisting load of a crane with a wide load-torque range and because the crane motion is typically started with a load, the motor's rated power is generally greater than the actual operating power, especially during a working cycle [3], [4]. Furthermore, the motor of the lifting mechanism usually operates with a light load, with no load, or with generating electricity [5]. Thus, a high-power motor drives a small load [6]. Furthermore, the motor runs under a constant voltage power supply, so the motor energy consumption is high, and electricity waste will inevitably occur [7]–[9]. Therefore, based on the operation characteristics of unknown and changing constant-torque load driven by the motor, it is of great practical significance to study its energy-saving principles and determine the corresponding energy-saving method. The paper [10] proposed a sectional control strategy integrating variable frequency with voltage regulation based on the mechanical load characteristics of the beam pumping motor system.

For the loads of fans and general pumps, if the motor adopts a speed regulation method, such as frequency conversion or pole change speed regulation, it not only achieves

The associate editor coordinating the review of this manuscript and approving it for publication was Tao Wang.

motor speed control but also has significant energy-saving effects [11], [12]. For the crane motor driving system with characteristics of constant-torque and variable-working loads, motor speed regulation is adopted to allow the motor to quickly track the load torque and achieve energy-saving effects. There are mainly two speed regulation modes: variable frequency speed regulation and pole-changing speed regulation based on the motor steady-state mathematical model [13], [14]. The latter is vector control based on a dynamic mathematical model of the motor [15], [16]. Vector control theories and methods mainly include adaptive control [17]–[20], inverse dynamics control [21]–[23], fuzzy control [24], [25], back-stepping control [26], and sliding mode control [27]–[29]. However, these energy-saving methods and measures aimed at regulating the motor speed have no significant energy-saving effects, and the designs of these controllers are more complex. Furthermore, the controller must collect more information about the state variables of the motor system during operation, so the use cost is relatively high.

If the load and working conditions of the motor vary greatly during a working cycle, the input stator voltage can be adjusted based on the motor's actual load, i.e., stator voltage regulation, which is a practical and effective energy saving method [30]. Energy saving controllers based on motor speed regulation must collect more motor system state variable information [31]. In comparison, stator voltage-regulating energy-saving methods only must adjust the input of the stator voltage based on the actual load, and thus, they only need information about motor's load torque. Therefore, the voltage energy-saving method is simpler and cheaper.

To achieve voltage regulation and energy savings of the motor, in general, maximum efficiency or minimum loss of the motor can be selected as the objective function [32], [33]. For a motor drive system such as crane, because of the wide range of loads and variable-working load characteristics, if there is a gradual transition from the motor state to the generator state for the lifting motor, the motor output power will change from positive to negative. The motor input power from the power grid absorption will also change from positive to negative, and the power input will even be less than the power output. The efficiency of the crane motor will change from a positive value less than 1 to a negative value or even to a value greater than 1. Therefore, it is not appropriate to choose the maximum efficiency as the control objective function of the voltage regulation and energy savings. Instead, the motor loss should be chosen as the control objective function for voltage regulation and energy savings.

To minimize the motor's total electrical loss (hereinafter referred to as the total electrical loss), the objective function of the total electrical loss of the motor must be minimized by adjusting the balance between the stator and rotor copper loss and the stator iron loss in the total electrical loss [34]–[36]. To achieve this goal, the paper [37] established an electrical loss objective function for non-uniform loads and used the Euler–Lagrange equation to determine the optimal voltage. The paper [38] directly solved the optimal voltage based on the specific slip. The paper [39] and [40] studied the voltage regulation and energy savings of motors with periodic load changes. For the paper [41], the electromagnetic power of the motor is used to calculate the optimal operating voltage value, but it is difficult to measure the electromagnetic power in actual operation. Therefore, in Reference 1, the optimal stator voltage is indirectly calculated by measuring the input power of the motor and the stator voltage. Existing problems: (1) increased the complexity of the calculation; (2) the optimal stator voltage itself is the result that needs to be calculated. However, Eqs. (6–7) in Reference 1 are contradictory to a certain extent by using the stator voltage of the motor during operation to calculate the optimal stator voltage of the motor. Essentially, the principle of establishing the objective function of the electrical total loss [37]–[41] is to decompose the total electrical loss into the invariable loss only related to the stator voltage (the stator copper consumption) and the variable loss only related to the load of the motor (the rotor copper consumption). In fact, when the motor drives a constant-torque load, if the principle above is applied to establish the objective function of the total electrical loss and determine the optimal voltage, the calculation process cannot be simplified. Determining how to further simplify the calculation process is the subject of this study. On the basis of the abovementioned studies, according to the induction motor Ã-type equivalent circuit [42], the stator copper loss will be regarded as an invariable loss associated with the stator voltage, and the stator iron loss will be regarded as an invariable loss associated with the stator voltage (this is different from previous studies [37]–[41] and is the innovation of this work). The rotor copper loss will be regarded as a variable loss that changes according to the variable load. The total electrical loss including the sum of the invariable and variable losses is established, and the relationship between the electrical total loss, stator voltage, and load torque is further obtained. The motor stator optimal regulation voltage is obtained through a simplified calculation. By comparing the energy consumption of the crane motor with that of the constant-voltage power supply, it was shown that a motor operating with the optimal regulation voltage based on a changing load torque exhibited a significant energy-saving effect. Particularly, compared with the experimental results in the paper [10], the calculation process in this paper is simple. Especially when the motor's load is light, it has a smaller total electrical loss (see Fig. 13).

II. ELECTRICAL LOSS BASED ON T-TYPE EQUIVALENT CIRCUIT OF MOTOR

The power flow diagram of the induction motor is shown in Figure 1. Through the air-gap magnetic field and electromagnetic coupling, the motor absorbs power from the grid power supply P_1, i.e., the motor's input power. P_1 is transformed into the motor rotor shaft output power P_2. The energy loss includes the stator copper loss P_{Cu1}, rotor copper loss P_{Cu2}, stator iron loss P_{Fe}, mechanical consumption P_{mec},

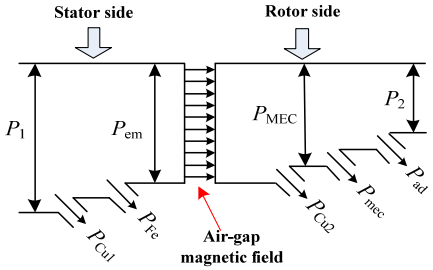

FIGURE 1. Power flow diagram of induction motor.

and additional loss P_{ad} on the motor rotor. P_{mec} and P_{ad} can be included in the mechanical power of the load, including the friction loss of the motor bearing, the ventilation loss caused by the fan, and the brush friction loss for the wound rotor, which are related to the structural design of the motor itself. These are outside the scope of this study. The total electrical loss of the motor is denoted as $\Sigma P_j = P_{mec} + P_{ad}$. The total mechanical loss of the motor is denoted as $\sum P = P_{\mathrm{Cu1}} + P_{\mathrm{Cu2}} + P_{\mathrm{Fe}}$. The electromagnetic power P_{em} after subtracting the stator copper consumption P_{Cu1} and the stator iron consumption P_{Fe} is denoted as $P_{em} = P_1 - (P_{Cu1} + P_{Fe})$. P_{em} is transmitted to the rotor side through the air-gap magnetic field. The remaining power after subtracting P_{Cu1}, P_{Fe}, and P_{Cu2} from P_1 is the motor's total mechanical power P_{MEC}, $P_{MEC} = P_{em} - P_{Cu2}$, i.e., $P_{MEC} = P_2 + P_{mec} + P_{ad}$. As shown in Figure 2, P_{Cu1}, P_{Cu2}, and P_{Fe}, which constitute the total electrical loss P, are defined as the product of the m_1-phase stator winding resistance R_1, the rotor winding resistance R'_2, and the excitation resistance R_{m}, respectively. These are calculated as follows:

$$\begin{cases} P_{\mathrm{Cu1}} = m_1 I_1^2 R_1 \\ P_{\mathrm{Cu2}} = m_1 I_2'^2 R'_2 \\ P_{\mathrm{Fe}} = m_1 I_0^2 R_{\mathrm{m}} \end{cases} . \tag{1}$$

The electrical losses associated with the passing currents are highlighted by rectangles in the T-type equivalent circuit shown in Fig. 2.

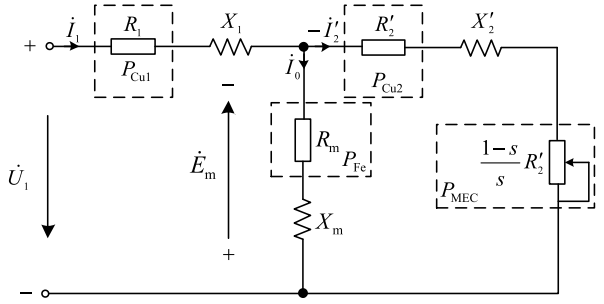

FIGURE 2. T-type equivalent circuit of induction motor.

If magnetic saturation is not taken into account, the power consumed by the excitation resistance R_{m}, namely the iron consumption P_{Fe}, is proportional to the square of the excitation electromotive force E_{m}^2. Generally, E_{m} is close to the stator voltage U_1 and remains constant, so the iron loss is considered to be an invariable loss. The rotor current $-I'_2$ increases with the increase in the slip s or the load carried by the rotor. The rotor copper consumption P_{Cu2} is a completely variable loss as the motor load changes. When the motor is operating under power generation conditions, s has a negative value and the rotor current is in the reverse phase. However, there is still loss. The stator current varies as the rotor current changes, so the stator copper loss P_{Cu1} is usually considered to be a variable loss. According to (1), the total electrical loss can be described as follows:

$$\sum P = m_1(I_1^2 R_1 + I_2'^2 R'_2 + I_0^2 R_{\mathrm{m}}). \tag{2}$$

III. ELECTRICAL LOSS BASED ON MOTOR Γ-TYPE EQUIVALENT CIRCUIT

Fig. 2 shows that the stator current vector is essentially the vector sum $\dot{I}_1 = \dot{I}_0 - \dot{I}'_2$ of the rotor current I'_2 and the excitation current I_0. Based on the analysis above, the rotor current depends on the load of the motor, and the excitation current mainly depends on the stator voltage, i.e., the stator copper consumption has an invariable loss caused by the excitation current component that changes with the load, which can be expressed as follows:

$$P_{\mathrm{Cu1}} = m_1(I_0 - I'_2)^2 R_1. \tag{3}$$

To study the invariable loss component of the stator copper consumption, the direct relationship between total electrical loss $\sum P$, stator voltage U_1, and load torque T_{L} is obtained. We considered an induction motor Γ-type circuit that is equivalent to the circuit shown in Fig. 2. In other words, the excitation branch in Fig. 2 is directly moved to the power end, and the complex correction coefficient C_1 is introduced. We define the following: modified reactance $X''_1 = C_1 X_1, X''_2 = C_1^2 X'_2$, modified resistor $R''_1 = C_1 R_1$, $R''_2 = C_1^2 R'_2$, and modified current $\dot{I}''_2 = \frac{\dot{I}'_2}{C_1}$. These are shown in Figure 3.

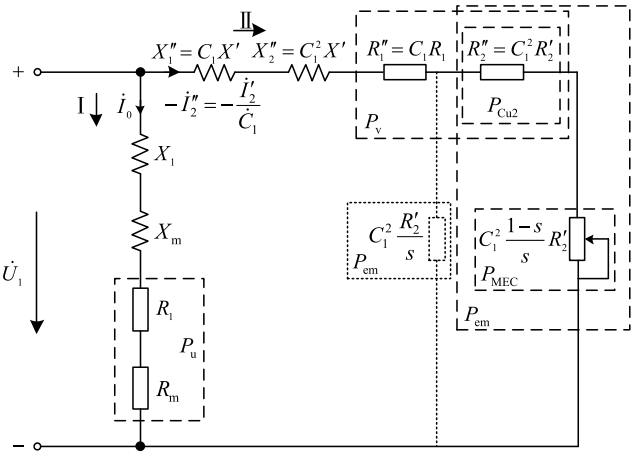

FIGURE 3. Γ-type equivalent circuit of induction motor.

For branch I, if magnetic saturation is not taken into account, when the stator voltage is constant, the losses due to resistance R_1 and R_m can be expressed as

$$P_u = m_1 r U_1^2, \tag{4}$$

where r is the equivalent conductance of branch I, and $r = \frac{R_1+R_m}{(R_1+R_m)^2+(X_1+X_m)^2}$.

Fig. 3 shows that P_u represents the invariable iron loss and stator copper loss caused by excitation current I_0. Equation (4) shows that P_u is only related to the stator voltage, so P_u is called the invariable loss of the motor. Correspondingly, branch I is called the constant loss branch, and branch II is called the variable loss branch.

For branch II, the loss of $C_1^2 R_2'$ is

$$m_1 I_2''^2 C_1^2 R_2' = m_1 I_2'^2 R_2' = P_{Cu2} \tag{5}$$

This corresponds to the rotor copper consumption P_{Cu2} in Fig. 2.

Similarly, the power consumed over resistance $C_1^2 \frac{1-s}{s} R_2'$ is

$$m_1 I_2''^2 C_1^2 \frac{1-s}{s} R_2' = m_1 I_2'^2 \frac{1-s}{s} R_2' = P_{MEC}. \tag{6}$$

This corresponds to the total mechanical power P_{MEC} in Fig. 2.

According to the power flow of the induction motor shown in Fig. 1 and Eqs. (5) and (6), the electromagnetic power of the induction motor is

$$P_{em} = P_{MEC} + P_{Cu2} = m_1 I_2''^2 C_1^2 \frac{R_2'}{s}. \tag{7}$$

From (7), we can obtain the following expression:

$$I_2''^2 = \frac{P_{em}}{m_1 C_1^2 R_2'/s}. \tag{8}$$

From the relationship between the torque, power, and angular velocity, we can obtain the following expression:

$$P_{em} = T_{em}\omega_1. \tag{9}$$

Therefore, the power consumed by the modified resistors R_1'' and R_2'' is defined as the variable loss P_v, which varies with the modified current I_2'', i.e.,

$$P_v = m_1 I_2''^2 (R_1'' + R_2''). \tag{10}$$

From Eqs. (8), (9), and (10), we obtain the following expression:

$$P_v = T_{em}\omega_1 \frac{R_1'' + R_2''}{R_2''/s}, \tag{11}$$

where ω_1 is the motor's synchronous angular velocity, $\omega_1 = 2\pi n_1/60$, $n_1 = 60 f_1/p$ is the synchronous speed, f_1 is the frequency of the power supply, and p is the motor's number of pole pairs.

Equation (11) shows that the variable loss P_v of the motor is only related to the load torque T_L, so it is reasonable to define it as the variable loss. Based on the division of the losses shown in Fig. 3, the total electrical loss of the induction motor is the sum of the invariable and variable losses, i.e.,

$$\begin{aligned}\sum P &= P_u + P_v \\ &= m_1 r U_1^2 + \omega_1 s \frac{R_1'' + R_2''}{R_2''} T_L.\end{aligned} \tag{12}$$

Equation (12) expresses the total electrical loss $\sum P$ based on the induction motor's Γ-type equivalent circuit when the motor is running stably. Equation (12) shows the relationship between the total electrical loss $\sum P$, the motor stator voltage U_1, and the motor load torque T_L. Compared with (2), the objective function of the total electrical loss given by (12) has clearer electrical and physical interpretations, which can facilitate the direct analysis and optimization of the motor's voltage regulation and energy savings.

IV. OPTIMAL REGULATING VOLTAGE OF MOTOR ENERGY SAVING

In (12), since the slip s varies with the change of the motor load torque T_L, T_L is used to represent s for calculation convenience. According to the variable loss branch II shown in Fig. 3 and (9), when the motor is in steady-state operation, $T_{em} = T_L$, the torque is expressed as follows:

$$\begin{aligned}T_{em} &= \frac{m_1 U_1^2}{(R_1'' + R_2''/s)^2 + (X_1'' + X_2'')^2} \cdot \frac{R_2''/s}{\omega_1} \\ &= \frac{m_1 U_1^2 \cdot s R_2''}{\omega_1 \{R_2''^2 + 2 s R_1'' R_2'' + s^2 [R_1''^2 + (X_1'' + X_2''^2)]\}}.\end{aligned} \tag{13}$$

In this case, $0 < s < 1$, so s can be solved in (13):

$$\begin{aligned}s &= \{[m_1 U_1^2 - 2\omega_1 R_1'' T_L \\ &\to -\sqrt{m_1^2 U_1^4 - 4 m_1 U_1^2 \omega_1 R_1'' T_L - 4\omega_1^2 (X_1'' + X_2'')^2 T_L^2}] \\ &\to R_2''\} \cdot \{2\omega_1 [R_1''^2 + (X_1'' + X_2'')^2] T_L\}^{-1}.\end{aligned} \tag{14}$$

In (14), s is accurately expressed by T_L. When the motor operates at steady state, s^2 is very small (generally 0.0001–0.0009). After neglecting $s^2[R_1''^2 + (X_1'' + X_2'')^2]$ in the denominator of (13), the approximate torque can be obtained when the slip $s = 0.01$–0.03, as follows:

$$\tilde{T}_L = \frac{m_1 U_1^2 \cdot s R_2''}{\omega_1 (R''^2 + 2 s R_1'' R_2'')}. \tag{15}$$

The error of the load torque calculated by (15) generally does not exceed 2 N·m (the approximate solution is verified in Section 5.1), which is a permissible error for engineering applications. Thus, the following approximate expression for s can be obtained from (15):

$$\tilde{s} = \frac{\omega_1 R_2'' T_L}{m_1 U_1^2 - 2\omega_1 R_1'' T_L}. \tag{16}$$

By substituting (14) into (12), the total electrical loss of the motor can be accurately represented by the stator voltage U_1 and motor load torque T_L, i.e., the exact solution $\sum P$ of the total electrical loss. By substituting (16) into (12), the total

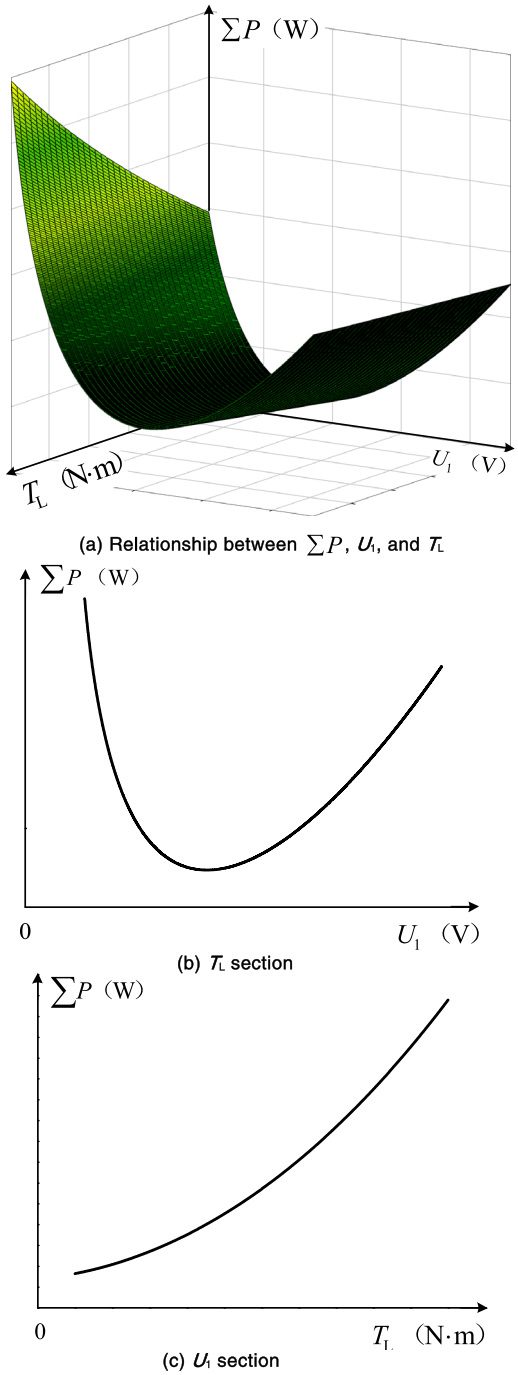

FIGURE 4. Relationship between the total electrical loss, stator voltage, and load torque.

electrical loss of the motor can be expressed approximately by the stator voltage and motor load torque, i.e., the approximate solution $\sum \tilde{P}$ of the total electrical loss. The approximate expression (16) is convenient to use and significantly simplifies the calculation.

Based on the approximate expression of the total electrical loss, the relationship between $\sum P$, U_1, and T_L can be obtained, as shown in Figure 4, where Fig. 4(b) and (c) show the T_L and U_1 sections, respectively. As shown in Fig. 4, when the parameters of the induction motor are determined, the stator voltage U_1 and load torque T_L will affect the total electrical loss. When the load torque T_L applied to the rotor is constant, there must be a minimum stator voltage to minimize the electrical total loss. When the stator voltage U_1 is constant, the total electrical loss increases with the increase in the load torque T_L. The stator voltage that minimizes the total electrical loss is called the optimal regulating voltage for the energy-saving operation of the induction motor, denoted as U_1^*.

To optimize the voltage regulation and energy savings, an appropriate voltage must be supplied to the induction motor stator under a certain load torque, so that the objective function given by (12) of the total electrical loss can be minimized. To facilitate the calculation and avoid complicated calculations, we can obtain a differential expression for $\sum P$ with respect to U_1 from Eqs. (12) and (15):

$$\frac{\mathrm{d}\sum P}{\mathrm{d}U_1} = 2m_1 r U_1 - \frac{2T_L^2\omega_1^2 m_1(R_1'' + R_2'')U_1}{(2T_L\omega_1 R_1'' - m_1 U_1^2)^2}. \tag{17}$$

We let $\frac{\mathrm{d}\sum P}{\mathrm{d}U_1} = 0$, and the optimal voltage of the motor energy saving can be obtained:

$$U_1^* = \begin{cases} \sqrt{\dfrac{(2R_1'' + \sqrt{\dfrac{R_1''+R_2''}{r}})\omega_1 T_L}{m_1}} & T_L > 0 \\ \sqrt{\dfrac{(2R_1'' - \sqrt{\dfrac{R_1''+R_2''}{r}})\omega_1 T_L}{m_1}} & T_L < 0 \end{cases}. \tag{18}$$

When $T_L > 0$, the motor is in an operating state of electrical. When $T_L < 0$, the motor is in a state of power generation. There are always mechanical and additional losses (as shown in Fig. 1) when the motor is running, and they are all taken into account in the load torque T_L, so $T_L \neq 0$. Therefore, to ensure the normal operation of the motor, $U_1 \neq 0$.

The influence of the stator voltage on the variation rate of the total electrical loss is shown in Figure 5. When $U_1 < U_1^*$, the electrical total loss decreased rapidly first and then slowly with the increase in U_1. When $U_1 \geq U_1^*$, the total electrical loss increased slowly with the increase in U_1.

Neglecting the motor's power generation operating conditions, we define

$$U_1^* = \alpha\sqrt{T_L}, \tag{19}$$

and $\alpha = \sqrt{\frac{(2R_1'' + \sqrt{\frac{R_1''+R''}{r}})\omega_1}{m_1}}$. α is called the optimal voltage regulating coefficient of the motor energy savings. When the power supply frequency f_1 is determined, α is only related to the motor's electrical parameters. When these electrical parameters and load torque are determined, the optimal voltage regulation is determined.

By substituting (15) into (19), the approximate solution $\tilde{U}_1^*$ for the optimal voltage regulation can be obtained. As shown in (19), U_1^* changes exponentially with the load torque of

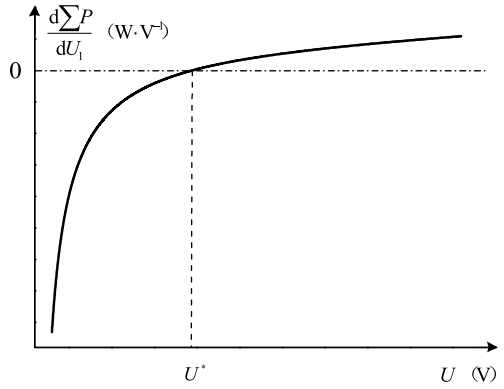

FIGURE 5. Influence of stator voltage on the variation rate of total electrical loss.

the motor. By substituting (19) into (12), we can obtain the minimum total electrical loss:

$$\min \sum P = [2rR_1'' + \sqrt{r(R_1'' + R_2'')} + \frac{R_1'' + R_2''}{R_2''/s}]\omega_1 T_L. \quad (20)$$

Further, we can obtain the following expression:

$$\min \sum P = [2rR_1'' + \sqrt{r(R_1'' + R_2'')} \rightarrow + \frac{R_1'' + R_2''}{30\omega_1 R_2''}(30\omega_1 - \pi n)]\omega_1 T_L. \quad (21)$$

According to Eq. (21), when the motor operates at the optimal voltage U_1^* and its parameters are determined, its speed n and load torque T_L together affect the minimum electrical total loss $\min \sum P$.

V. CALCULATION EXAMPLE

A. APPROXIMATE SOLUTION VERIFICATION

To verify the effectiveness and energy-saving effect of the optimal voltage regulation and the energy saving principle of the motor proposed in this study, a three-phase, six-pole cage motor used in a TJLQ30.5b railway container gantry crane was taken as an example. The motor parameters were as follows: $R_1 = 1.375\Omega$, $X_1 = 2.430\Omega$, $R_2' = 1.047\Omega$, $X_2' = 4.400\Omega$, $R_m = 8.340\Omega$, $X_m = 82.600\Omega$, the rated slip $s_N = 0.0298$, the rated speed $n_N = 980\text{r} \cdot \text{min}^{-1}$, the rated power $P_N = 5.5\text{kW}$ and the rated torque $T_N = 50N \cdot m$.

When $s^2 = 0.0001$–0.0009, i.e. $s = 0.01$–0.03, the exact solution T_L and approximate solution $\tilde{T}_L$ of the motor load torque varying with slip were calculated using Eqs. (13) and (15), respectively, and the load torque error ($\delta(T_L) = \tilde{T}_L - T_L$) is shown in Figure 6. Fig. 6 shows that the load torque error of the motor increased with the increase in the slip s, but within the range of s, the load torque error of the motor did not exceed 1.8 N·m.

Similarly, based on the exact solution (14), the approximate solution (16) of s, and (12), the variation of the approximate solution $\sum \tilde{P}$, the exact solution $\sum P$, and the error ($\delta(\sum P) = \sum \tilde{P} - \sum P$) curves with the stator voltage were calculated, as shown in Figure 7. When the voltage regulation

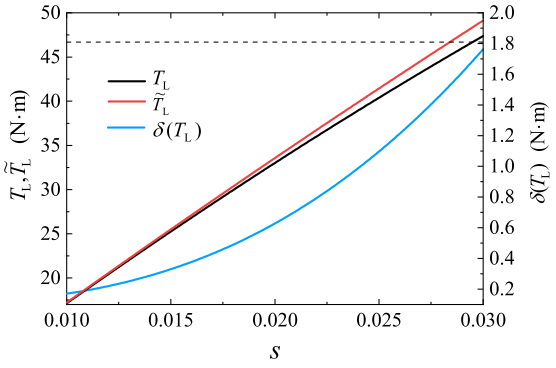

FIGURE 6. Comparison of load torque's calculation results.

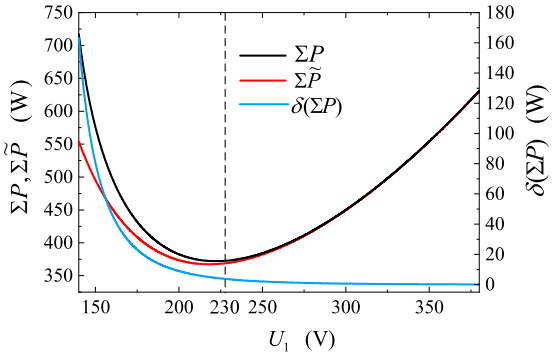

FIGURE 7. Comparison of total electrical loss calculation results.

was lower than 230 V, the total electrical loss error was relatively large. When the voltage regulation was higher than 230 V, the total electrical loss error was almost 0. Because the working voltage of a crane motor is generally higher than 220 V, the approximate solution of the slip s can be used, and there is almost no total electrical loss error.

According to Eqs. (14) and (16), the optimal voltage regulation results using the approximate solution $\tilde{U}_1^*$, exact solution U_1^*, and the optimal voltage regulation error ($\delta(U_1^*) = \tilde{U}_1^* - U_1^*$) (based on the exact and approximate solutions of the slip s) with the change of the crane motor load torque were calculated, as shown in Figure 8. The optimal voltage regulation error increased with the increase in the crane motor load torque. However, within the working voltage range of the crane motor, the optimal voltage regulation error did not exceed 6 V.

Therefore, ignoring $s^2[R_1''^2 + (X_1'' + X_2'')^2]$ in (13), it is reasonable and effective to calculate the motor load torque and optimal voltage regulation based on the approximate solution of the slip s, and the solution process is also simplified.

B. ANALYSIS OF OPTIMAL VOLTAGE REGULATION AND ENERGY-SAVING EFFECT

To verify the energy-saving effect of the optimal voltage regulating method, based on the operating characteristics of a motor with a constant torque load and different percentages of the motor's rated torque (load rate), the motor's load was

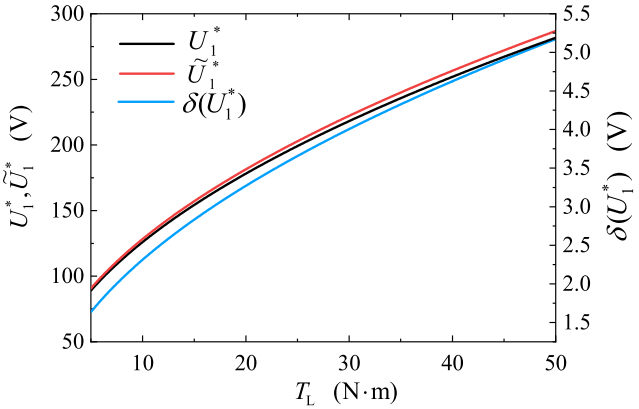

FIGURE 8. Comparison of optimal voltage regulation calculation results.

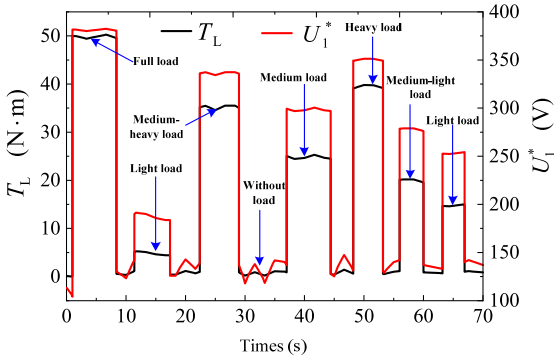

FIGURE 9. Motor load torque and optimal voltage regulation.

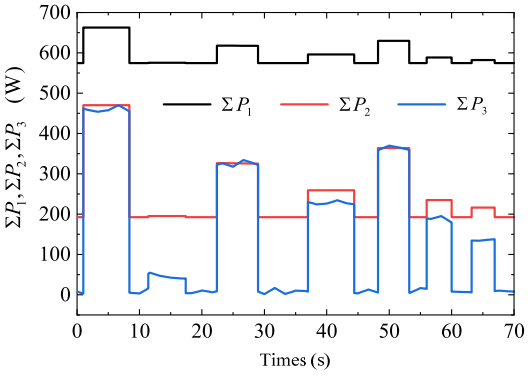

FIGURE 10. Comparison of total electrical loss of motor.

divided into a light load ($T_L \leq 0.3T_N$), medium-light load ($0.3T_N < T_L < 0.5T_N 0.3\mathrm{T_N} < \mathrm{T_L} < 0.5\mathrm{T_N}$), medium load ($T_L = 0.5T_N \mathrm{T_L} = 0.5\mathrm{T_N}$), medium-heavy load ($0.5\mathrm{T_N} < \mathrm{T_L} < 0.8\mathrm{T_N} 0.5T_N < T_L < 0.8T_N$), heavy load ($0.8T_N \leq T_L < T_N$), and full load ($\mathrm{T_L} = \mathrm{T_N} T_L = T_N$). Assuming that the load torque fluctuates to a certain extent, the load torque curve of the motor within a certain operating cycle and the optimal voltage regulation curve were calculated using (19) and are shown in Figure 9. Equation (12) can be used to calculate the total electrical losses for 380 and 220 V. Equation (20) was used to calculate the total electrical loss of the optimal voltage regulation, as shown in Figure 10. The following conclusions were drawn from Fig. 10. The total electrical

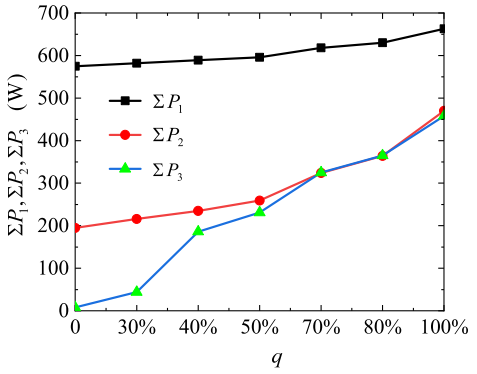

FIGURE 11. Influence of motor load rate on total electrical loss.

loss of the motor driven by a 380-V constant voltage was the largest throughout the operation cycle. With the variation of the load, the total electrical loss fluctuated within a certain range. When the motor was driven by a 380-V constant voltage, the fluctuation range of the total electrical loss was about $\sum P_1 = 570 - 663W$. When the motor was driven by a 220-V constant voltage, the fluctuation range of the total electrical loss was about $\sum P_2 = 192 - 470W$. When the motor was driven by the optimal voltage regulation, the fluctuation range of the total electrical loss was about $\sum P_3 = 8 - 458W$.

The curves in Fig. 10 were further represented as the relationship between the total electrical loss and load rate q, as shown in Figure 11. The following conclusions were drawn from Fig. 11. When the load rate was $q \leq 70\%$, i.e., the crane did not exceed the medium-heavy-load operation, and the total electrical loss of the optimal voltage-regulating drive was less than the total electrical loss of the 220-V constant voltage drive. In this case, the crane showed a significant energy-saving effect. When the load rate was $q > 70\%$, i.e., when the crane operated under the medium-heavy, heavy, or full load, the total electrical loss was almost equal to that under a 220-V constant voltage drive. The total electrical loss increased with the increase in the load rate q. However, the total electrical loss did not increase significantly when driven by a 380-V constant voltage, but it increased significantly when driven by the optimal voltage regulation.

When the motor operates with the optimal regulated voltage, the combined influence of the motor speed and load on the minimum total electrical loss is shown in Fig. 12. It can also be seen from Fig. 12 that the motor has an obvious energy-saving effect in the region of medium load and rated speed, which further verifies that the optimal voltage regulation method proposed in this paper has an obvious energy-saving effect when the motor is dragging light load.

Fig. 13 shows the comparative results of the energy saving effect of the method adopted in this paper and the method in the paper [10]. It can be further seen that the optimal voltage regulation's energy-saving method adopted in this paper has a small total electrical loss when light load is applied.

When the motor did not exceed the medium load and operated with optimal voltage regulation, the energy-saving effect

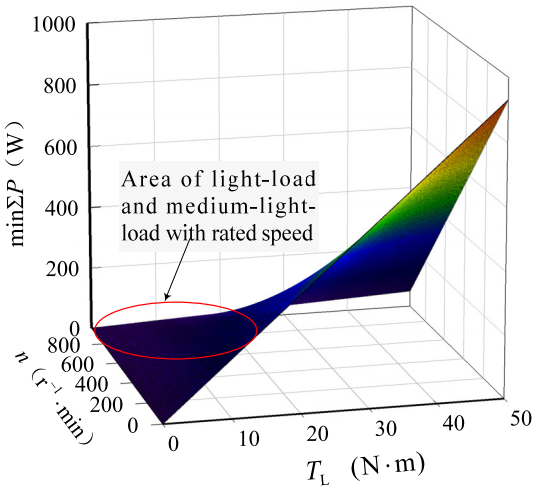

FIGURE 12. Total electrical loss varying with the speed and load torque.

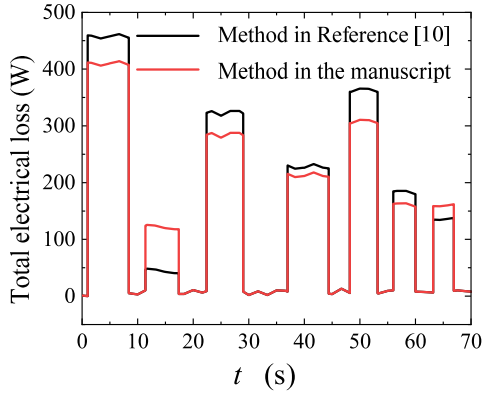

(a) Comparison of total electrical losses

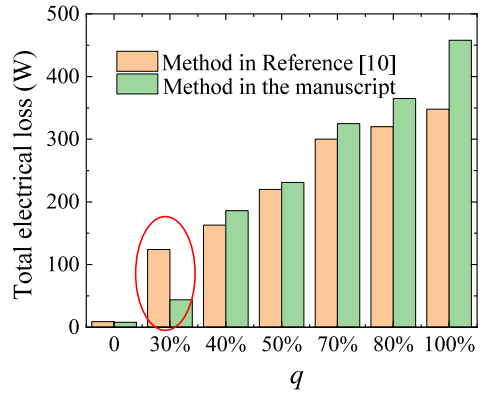

(b) Comparison of total electrical losses with different load rates

FIGURE 13. Comparison results between methods in this paper and Reference [10].

was significant. In particular, when the motor ran without a load, its total electrical loss was almost 0.

VI. CONCLUSION

Because an induction motor drive system operates with constant-torque and variable-working loads, the energy-saving effect based on speed regulation is not significant. To achieve optimal voltage regulation and energy savings of a motor during constant-torque and variable-working-load operations, a T-type and Γ-type equivalent circuit of an induction motor was established. The copper and iron losses of the stator were regarded as invariable losses that were only related to the stator voltage, and the copper losses of the rotor were regarded as variable losses that varied with the load torque. We deduced the electrical total loss formula $\sum P = m_1 r U_1^2 + \omega_1 s \frac{R_1'' + R_2''}{R_2''} T_L$ and the optimal voltage regulation formula $U_1^* = \alpha\sqrt{T_L}$ for an induction motor. Through these formulas and an engineering example, the following important conclusions were drawn.

(1) When the parameters of the induction motor are determined, the stator voltage U_1 and load torque T_L will affect the total electrical loss. When the load torque T_L applied to the rotor is constant, there must be an optimal voltage regulation U_1^* to minimize the total electrical loss. The optimal voltage regulation changes exponentially with the load torque of the motor. When $U_1 < U_1^*$, the total electrical loss decreased rapidly first and then slowly with the increase in U_1. When $U_1 \geq U_1^*$, the total electrical loss increased slowly with the increase in U_1.

(2) When slip $s = 0.01$–0.03 and the motor operated stably, the motor load torque error did not exceed 1.8 N·m based on the exact and approximate solutions of the slip s, and the total electrical loss had almost no calculation error when the working voltage of the motor was higher than 230 V.

(3) When the motor operated stably, the optimal voltage regulation and its error calculated using the exact and approximate solutions of the slip s increased with the increase in the motor load torque. However, within the working voltage range of the motor, the optimal voltage regulation error did not exceed 6 V.

(4) The total electrical loss of the motor driven by a 380-V constant voltage was the largest throughout the motor's operation cycle. With the change of the motor load, the total electrical loss fluctuated within a certain range. When the motor was driven by the optimal voltage regulation, the total electrical loss fluctuation range was the largest.

(5) With the increase in the load rate, the total electrical loss increased. However, the total electrical loss did not increase significantly when the motor was driven by a 380-V constant voltage. It increased significantly when the motor was driven by the optimal voltage regulation. When the motor's load did not exceed a medium load and the motor operated with the optimal voltage regulation, the energy-saving effect was significant. In particular, when the motor operated without a load, the total electrical loss of the motor was almost 0.

ACKNOWLEDGMENT

The authors thank the anonymous reviewers and editors for their prolific comments which significantly improved the quality of their work.

REFERENCES

[1] A. G. de Araujo Cruz, R. D. Gomes, F. A. Belo, and A. C. L. Filho, "A hybrid system based on fuzzy logic to failure diagnosis in induction motors," *IEEE Latin Amer. Trans.*, vol. 15, no. 8, pp. 1480–1489, Jul. 2017, doi: 10.1109/TLA.2017.7994796.

[2] B. Tekgun, Y. Sozer, and I. Tsukerman, "Modeling and parameter estimation of split-phase induction motors," *IEEE Trans. Ind. Appl.*, vol. 52, no. 2, pp. 1431–1440, Mar./Apr. 2016, doi: 10.1109/TIA.2015.2504417.

[3] N. Sun, Y. Wu, H. Chen, and Y. Fang, "An energy-optimal solution for transportation control of cranes with double pendulum dynamics: Design and experiments," *Mech. Syst. Signal Process.*, vol. 102, pp. 87–101, Mar. 2018, doi: 10.1016/j.ymssp.2017.09.027.

[4] S. Pietrosanti, F. Alasali, and W. Holderbaum, "Power management system for RTG crane using fuzzy logic controller," *Sustain. Energy Technol. Assessments*, vol. 37, pp. 1–16, Feb. 2020, doi: 10.1016/j.seta.2020.100639.

[5] F. Alasali, S. Haben, and W. Holderbaum, "Energy management systems for a network of electrified cranes with energy storage," *Int. J. Elect. Power Energy Syst.*, vol. 106, pp. 210–222, Mar. 2019, doi: 10.1016/j.ijepes.2018.10.001.

[6] T. Ho, K. Suzuki, M. Tsume, R. Tasaki, T. Miyoshi, and K. Terashima, "A switched optimal control approach to reduce transferring time, energy consumption, and residual vibration of payload's skew rotation in crane systems," *Control Eng. Pract.*, vol. 84, pp. 247–260, Mar. 2019, doi: 10.1016/j.conengprac.2018.11.018.

[7] M. Sha, T. Zhang, Y. Lan, X. Zhou, T. Qin, D. Yu, and K. Chen, "Scheduling optimization of yard cranes with minimal energy consumption at container terminals," *Comput. Ind. Eng.*, vol. 113, pp. 704–713, Nov. 2017, doi: 10.1016/j.cie.2016.03.022.

[8] J. He, Y. Huang, W. Yan, and S. Wang, "Integrated internal truck, yard crane and quay crane scheduling in a container terminal considering energy consumption," *Expert Syst. Appl.*, vol. 42, no. 5, pp. 2464–2487, Apr. 2015, doi: 10.1016/j.eswa.2014.11.016.

[9] Z. Shang, D. Gao, Z. Jiang, and Y. Lu, "Towards less energy intensive heavy-duty machine tools: Power consumption characteristics and energy-saving strategies," *Energy*, vol. 178, pp. 263–276, Jul. 2019, doi: 10.1016/j.energy.2019.04.133.

[10] Y. Wang, H. H. Eldeeb, H. Zhao, and O. A. Mohammed, "Sectional variable frequency and voltage regulation control strategy for energy saving in beam pumping motor systems," *IEEE Access*, vol. 7, pp. 92456–92464, 2019, doi: 10.1109/ACCESS.2019.2927525.

[11] B. Capelo, M. Pérez-Sánchez, J. F. P. Fernandes, H. M. Ramos, P. A. López-Jiménez, and P. J. C. Branco, "Electrical behaviour of the pump working as turbine in off grid operation," *Appl. Energy*, vol. 208, pp. 302–311, Dec. 2017, doi: 10.1016/j.apenergy.2017.10.039.

[12] S. Shukla and B. Singh, "Adaptive speed estimation with fuzzy logic control for PV-grid interactive induction motor drive-based water pumping," *IET Power Electron.*, vol. 12, no. 6, pp. 1554–1562, May 2019, doi: 10.1049/iet-pel.2018.5571.

[13] M. J. S. Zuberi, A. Tijdink, and M. K. Patel, "Techno-economic analysis of energy efficiency improvement in electric motor driven systems in swiss industry," *Appl. Energy*, vol. 205, pp. 85–104, Nov. 2017, doi: 10.1016/j.apenergy.2017.07.121.

[14] Y. Li, M. Liu, J. Lau, and B. Zhang, "A novel method to determine the motor efficiency under variable speed operations and partial load conditions," *Appl. Energy*, vol. 144, pp. 234–240, Apr. 2015, doi: 10.1016/j.apenergy.2015.01.064.

[15] S. Payami and R. K. Behera, "An improved DTC technique for low-speed operation of a five-phase induction motor," *IEEE Trans. Ind. Electron.*, vol. 64, no. 5, pp. 3513–3523, May 2017, doi: 10.1109/TIE.2017.2652397.

[16] N. Pimkumwong and M.-S. Wang, "Full-order observer for direct torque control of induction motor based on constant V/F control technique," *ISA Trans.*, vol. 73, pp. 189–200, Feb. 2018, doi: 10.1016/j.isatra.2017.12.014.

[17] D. Xu, J. Huang, X. Su, and P. Shi, "Adaptive command-filtered fuzzy backstepping control for linear induction motor with unknown end effect," *Inf. Sci.*, vol. 477, pp. 118–131, Mar. 2019, doi: 10.1016/j.ins.2018.10.032.

[18] H.-H. Chiang, K.-C. Hsu, and I.-H. Li, "Optimized adaptive motion control through an SoPC implementation for linear induction motor drives," *IEEE/ASME Trans. Mechatronics*, vol. 20, no. 1, pp. 348–360, Feb. 2015, doi: 10.1109/TMECH.2014.2313594.

[19] C. Fu, J. Yu, L. Zhao, H. Yu, C. Lin, and Y. Ma, "Barrier Lyapunov function-based adaptive fuzzy control for induction motors with iron losses and full state constraints," *Neurocomputing*, vol. 287, pp. 208–220, Apr. 2018, doi: 10.1016/j.neucom.2018.02.020.

[20] J. Talla, V. Q. Leu, V. Smidl, and Z. Peroutka, "Adaptive speed control of induction motor drive with inaccurate model," *IEEE Trans. Ind. Electron.*, vol. 65, no. 11, pp. 8532–8542, Nov. 2018, doi: 10.1109/TIE.2018.2811362.

[21] L. Rincon, Y. Kubota, G. Venture, and Y. Tagawa, "Inverse dynamic control via 'simulation of feedback control' by artificial neural networks for a crane system," *Control Eng. Pract.*, vol. 94, pp. 1–18, Jan. 2020, doi: 10.1016/j.conengprac.2019.104203.

[22] W. Bu and Z. Li, "LS-SVM inverse system decoupling control strategy of a bearingless induction motor considering stator current dynamics," *IEEE Access*, vol. 7, pp. 132130–132139, 2019, doi: 10.1109/ACCESS.2019.2939258.

[23] X. Sun, Z. Shi, L. Chen, and Z. Yang, "Internal model control for a bearingless permanent magnet synchronous motor based on inverse system method," *IEEE Trans. Energy Convers.*, vol. 31, no. 4, pp. 1539–1548, Dec. 2016, doi: 10.1109/TEC.2016.2591925.

[24] Z. Zhao, J. Yu, L. Zhao, H. Yu, and C. Lin, "Adaptive fuzzy control for induction motors stochastic nonlinear systems with input saturation based on command filtering," *Inf. Sci.*, vols. 463–464, pp. 186–195, Oct. 2018, doi: 10.1016/j.ins.2018.06.042.

[25] L. A. Mier, J. S. Benitez, R. López, J. A. Segovia, R. Peña, and F. J. Ramirez, "Adaptive fuzzy control system for a squirrel cage induction motor," *IEEE Latin Amer. Trans.*, vol. 15, no. 5, pp. 795–805, May 2017, doi: 10.1109/TLA.2017.7910191.

[26] K. Saad, K. Abdellah, H. Ahmed, and A. Iqbal, "Investigation on SVM-backstepping sensorless control of five-phase open-end winding induction motor based on model reference adaptive system and parameter estimation," *Eng. Sci. Technol., Int. J.*, vol. 22, no. 4, pp. 1013–1026, Aug. 2019, doi: 10.1016/j.jestch.2019.02.008.

[27] R. N. Mishra and K. B. Mohanty, "Development and implementation of induction motor drive using sliding-mode based simplified neuro-fuzzy control," *Eng. Appl. Artif. Intel.*, vol. 91, pp. 1013–1026, May 2020, doi: 10.1016/j.engappai.2020.103593.

[28] Z. Yang, D. Zhang, X. Sun, and X. Ye, "Adaptive exponential sliding mode control for a bearingless induction motor based on a disturbance observer," *IEEE Access*, vol. 6, pp. 35425–35434, Jun. 2018, doi: 10.1109/ACCESS.2018.2851590.

[29] A. Saghafinia, H. W. Ping, M. N. Uddin, and K. S. Gaeid, "Adaptive fuzzy sliding-mode control into chattering-free IM drive," *IEEE Trans. Ind. Appl.*, vol. 51, no. 1, pp. 692–701, Jan. 2015, doi: 10.1109/TIA.2014.2328711.

[30] V. S. Santos, J. J. C. Eras, A. S. Gutierrez, and M. J. C. Ulloa, "Assessment of the energy efficiency estimation methods on induction motors considering real-time monitoring," *Measurement*, vol. 136, pp. 237–247, Mar. 2019, doi: 10.1016/j.measurement.2018.12.080.

[31] D. M. Stojic, M. Milinkovic, S. Veinovic, and I. Klasnic, "Stationary frame induction motor feed forward current controller with back EMF compensation," *IEEE Trans. Energy Convers.*, vol. 30, no. 4, pp. 1356–1366, Dec. 2015, doi: 10.1109/TEC.2015.2438093.

[32] H.-C. Chuang, G.-D. Li, and C.-T. Lee, "The efficiency improvement of AC induction motor with constant frequency technology," *Energy*, vol. 174, pp. 805–813, May 2019, doi: 10.1016/j.energy.2019.03.019.

[33] Y. Deng, G. Zhao, X. Yi, and W. Xiao, "Contact modeling and input-voltage-region based parametric identification for speed control of a standing wave linear ultrasonic motor," *Sens. Actuators A, Phys.*, vol. 295, pp. 456–468, Aug. 2019, doi: 10.1016/j.sna.2019.06.016.

[34] M. Al-Badri, P. Pillay, and P. Angers, "A novel *in situ* efficiency estimation algorithm for three-phase induction motors operating with distorted unbalanced voltages," *IEEE Trans. Ind. Appl.*, vol. 53, no. 6, pp. 5338–5347, Nov. 2017, doi: 10.1109/TIA.2017.2728786.

[35] M. P. Shreelakshmi and V. Agarwal, "Trajectory optimization for loss minimization in induction motor fed elevator systems," *IEEE Trans. Power Electron.*, vol. 33, no. 6, pp. 5160–5170, Jun. 2018, doi: 10.1109/TPEL.2017.2735905.

[36] J. Titus, J. Teja, K. Hatua, and K. Vasudevan, "An improved scheme for extended power loss ride-through in a voltage-source-inverter-fed vector-controlled induction motor drive using a loss minimization technique," *IEEE Trans. Ind. Appl.*, vol. 52, no. 2, pp. 1500–1508, Mar./Apr. 2016, doi: 10.1109/TIA.2015.2488657.

[37] C. Ponmani and M. Rajaram, "Compensation strategy of matrix converter fed induction motor drive under input voltage and load disturbances using internal model control," *Int. J. Electr. Power Energy Syst.*, vol. 44, no. 1, pp. 43–51, Jan. 2013, doi: 10.1016/j.ijepes.2012.07.031.

[38] W. Li, V. Vaziri, S. S. Aphale, S. M. Dong, and M. Wiercigroch, "Dynamics and frequency and voltage control of downhole oil pumping system," *Mech. Syst. Signal Process*, vol. 139, pp. 1–24, May 2020, doi: 10.1016/j.ymssp.2019.106562.

[39] C.-Y. Zhang, L. Wang, and H. Li, "Optimization method based on process control of a new-type hydraulic-motor hybrid beam pumping unit," *Measurement*, vol. 158, pp. 43–51, Jul. 2020, doi: 10.1016/j.measurement.2020.107716.
[40] H. Zhao, Y. Wang, Y. Zhan, G. Xu, X. Cui, and J. Wang, "Practical model for energy consumption analysis of beam pumping motor systems and its energy-saving applications," *IEEE Trans. Ind. Appl.*, vol. 54, no. 2, pp. 1006–1016, Mar. 2018, doi: 10.1109/TIA.2017.2779103.
[41] R. Li and S. Li, "Energy-saving research on asynchronous motor voltage regulation using Γ equivalent circuit," in *Unifying Electrical Engineering and Electronics Engineering*. New York, NY, USA; Springer, 2014, pp. 833–839.
[42] X. Zhou, B. Yang, Y. Ma, and Z. Gao, "Research review on the energy-saving technologies for asynchronous motors," in *Proc. IEEE Int. Conf. Mechatronics Automat. (ICMA)*, Changchun, China, Aug. 2018, pp. 195–199, doi: 10.1109/ICMA.2018.8484643.

ZHONG BIN was born in Sichuan, China, in 1975. He received the B.E. and M.E. degrees in mechanical engineering from the College of Engineering and Technology (CET), Southwest University, Chongqing, China, in 2000 and 2005, respectively, and the Ph.D. degree in mechatronic engineering from the School of Mechanical Engineering, Southwest Jiaotong University, Chengdu, China, in 2007. He is currently a Professor and a Ph.D. Supervisor with the School of Mechanical Engineering, Chengdu University, Sichuan, China. His research interests include mechatronics, motion control, and intelligent robotic system applications.

MA LILI was born in Jiangsu, China, in 1980. She received the B.E. and M.E. degrees in mechanical engineering from the College of Engineering and Technology (CET), Southwest University, Chongqing, China, in 2002 and 2005, respectively, and the Ph.D. degree in mechatronic engineering from the School of Mechanical Engineering, Southwest Jiaotong University, Chengdu, China, in 2013. She is currently a Lecturer with the College of Equipment Management and Support, Engineering University of PAP. Her research interests include mechatronics, computer vision, and intelligent robots.

DONG HAO received the B.E. and Ph.D. degrees in mechanical engineering from the School of Mechanical Engineering, Southwest Jiaotong University, Chengdu, China, in 2008 and 2015, respectively. He is currently an Associate Researcher with the School of Mechanical Engineering, Chengdu University. He is a member of the Chinese Society of Mechanics.